

Received Date : 21-Aug-2012
Revised Date : 24-Oct-2012
Accepted Date : 25-Oct-2012
Article type : Primary Research Articles

Changes in satellite-derived spring vegetation green-up date and its linkage to climate in China from 1982 to 2010: a multi-method analysis

Nan Cong¹, Tao Wang², Huijuan Nan¹, Yuecun Ma¹,
Xuhui Wang¹, Ranga B. Myneni³, and Shilong Piao^{1,4*}

¹ College of Urban and Environmental Sciences, Sino-French Institute for Earth System Science, and Key Laboratory for Earth Surface Processes of the Ministry of Education, Peking University, Beijing 100871, China

² Laboratoire des Sciences du Climat et de l'Environnement, CEA CNRS UVSQ, 91191 Gif sur Yvette, France

³ Department of Geography and Environment, Boston University, 675 Commonwealth Avenue, Boston, MA 02215, USA

⁴ Institute of Tibetan Plateau Research, Chinese Academy of Sciences, Beijing 100085, China

Running title: Spring phenology change in China

Keywords: Climate Change, phenology, spring vegetation green-up date, temperature sensitivity of spring phenology, China

Manuscript for *Global Change Biology*

* **Corresponding author:**

Shilong Piao
Peking University
Beijing 100871, China
Tel: 86-10-6275-3298, Fax: 86-10-6275-1179
Email: slpiao@pku.edu.cn

This article has been accepted for publication and undergone full peer review but has not been through the copyediting, typesetting, pagination and proofreading process, which may lead to differences between this version and the Version of Record. Please cite this article as doi: 10.1111/gcb.12077

© 2012 Blackwell Publishing Ltd

Abstract

The change in spring phenology is recognized to exert a major influence on carbon balance dynamics in temperate ecosystems. Over the past several decades, several studies focused on shifts in spring phenology; however, large uncertainties still exist, and one under-studied source could be the method implemented in retrieving satellite-derived spring phenology. To account for this potential uncertainty, we conducted a multi-method investigation to quantify changes in vegetation green-up date from 1982 to 2010 over temperate China, and to characterize climatic controls on spring phenology. Over temperate China, the five methods estimated that the vegetation green-up onset date advanced, on average, at a rate of 1.3 ± 0.6 days per decade (ranging from 0.4 to 1.9 days per decade) over the last 29 years. Moreover, the sign of the trends in vegetation green-up date derived from the five methods were broadly consistent spatially and for different vegetation types, but with large differences in the magnitude of the trend. The large inter-method variance was notably observed in arid and semi-arid vegetation types. Our results also showed that change in vegetation green-up date is more closely correlated with temperature than with precipitation. However, the temperature sensitivity of spring vegetation green-up date became higher as precipitation increased, implying that precipitation is an important regulator of the response of vegetation spring phenology to change in temperature. This intricate linkage between spring phenology and precipitation must be taken into account in current phenological models which are mostly driven by temperature.

Keywords: Climate Change, phenology, spring vegetation green-up date, temperature sensitivity of spring phenology, China

Introduction

Vegetation phenology not only is a sensitive indicator of global climate change (Schwartz, 1998; Menzel & Fabian 1999), but also regulates climate change through its influences on the exchange of energy, water and carbon between land surface and atmosphere (Baldocchi *et al.*, 2001; Piao *et al.*, 2008; Peñuelas *et al.*, 2009; Richardson *et al.*, 2010). It has been suggested that longer growing seasons, particularly earlier spring vegetation green-up, significantly enhance vegetation productivity in the temperate and boreal regions (Keeling *et al.*, 1996; White *et al.*, 1999; Kimball *et al.*, 2004; Hu *et al.*, 2010). For example, multi-year eddy flux measurements of CO₂ exchange from an old-growth coniferous forest dominated by Norway spruce showed that annual gross primary productivity (GPP) increased by approximately 22 gC m⁻² for every 1 day earlier emergence of shoots in the month of May (Niemand *et al.*, 2005). Terrestrial carbon cycle models predict that on average, extension of vegetation growing season causes an increase in annual GPP by about 0.6% per day in the Northern Hemisphere (Piao *et al.*, 2007).

With the current trend of global warming (IPCC, 2007), significant changes in phenology have been widely observed (Cleland *et al.*, 2007; Jeong *et al.*, 2011; Zeng *et al.*, 2011). In particular, spring green-up advancements in response to a warming climate have been detected in many studies employing ground observations (e.g., Parmesan and Yohe 2003, Menzel *et al.*, 2006, Vitasse *et al.*, 2009) and satellite data (e.g., Zhou *et al.*, 2001, Piao *et al.*, 2006; White *et al.*, 2009). Despite the advancing trend of spring green-up onset suggested by most studies, the magnitudes of such advances vary substantially among

different studies, especially those based on satellite data sets. This large difference in the magnitude estimate cannot be attributed solely to regional or temporal differences, since it has also been found for the same region and same period in different studies. For instance, White et al. (2009) estimated the spring green-up onset in North America with 10 different methods, which yielded a deviation as large as ± 60 days. Moreover, our previous analyses (Cong *et al.*, 2012) also showed that there is large inter-method difference in spring green-up onset dates estimated by five different methods, and merits and pitfalls of specific method are dependent on vegetation type or physical environment. For example, in contrary to other methods, Timesat and Polyfit are relatively unstable at forest and grassland sites respectively. Thus, it is crucial to use different methods to compare the differences in changes in vegetation phenology.

Temperate China has experienced dramatic climate change (Piao *et al.*, 2010). Vegetation in this region has already changed in response to recent climatic changes including species migration and movement of vegetation boundaries (Parmesan 2006), vegetation productivity (Peng *et al.*, 2011), and phenology (Piao *et al.*, 2006; Jeong *et al.*, 2011). In the case of phenology, a growing body of evidence suggests that climate warming has advanced the biological spring in temperate China (Zheng *et al.*, 2002; Chen *et al.*, 2005; Piao *et al.*, 2006; Tao *et al.*, 2006). For example, using NOAA/AVHRR satellite derived normalized difference vegetation index (NDVI) data, Piao et al. (2006) reported that the spring phenology in temperate China advanced by 7.9 days per decade from 1982 to 1999. There is clearly a great deal of uncertainty regarding this spring phenological changes

inferred from satellite data. Our previous work showed that the standard deviation (SD) of the satellite data estimated spring onset dates from different methods is larger than 1 month in about 24% of the temperate China (Cong *et al.*, 2012). However, little is known about how trends in spring phenology over China are sensitive to the algorithm used to identify the start of the growing season. Furthermore, our understanding of the linkage between phenology and climate change in China is very limited, which further limit our ability to predict future phenology change under global warming (Fang *et al.*, 2002).

In this study, we employed five different methods to estimate the trends of spring green-up onset dates and their sensitivities to temperature changes for temperate China north of 30°N using NOAA/AVHRR NDVI data from 1982 to 2010. The objectives of this paper are to (1) systematically evaluate the uncertainties of satellite based spring vegetation green-up date changes, and (2) quantify the responses of spring onset dates to temperature change and its uncertainty in temperate China during the last three decades.

Materials and Methods

Dataset

The normalized difference vegetation index (NDVI) is obtained from red (R) and near-infrared (NIR) reflectance,

$$\text{NDVI} = (\text{Band}_{\text{NIR}} - \text{Band}_{\text{R}}) / (\text{Band}_{\text{NIR}} + \text{Band}_{\text{R}}) \quad (1)$$

where Band_{NIR} is the value of near-infrared band, and Band_{R} is the value of red band. NDVI is related to the absorption of photosynthetically active radiation by plant canopies (Asrar *et al.*,

1984), and is widely used in the studies of vegetation remote sensing (Tucker et al., 2005; Wang et al., 2011). In this study, we used an AVHRR (Advanced Very High Resolution Radiometer) NDVI data set developed by the Global Inventory Modeling and Mapping Studies (GIMMS) group at NASA Goddard Space Flight Center (NDVI3g dataset). The dataset, has a spatial resolution of 10 km and a temporal resolution of 15-day, available from 1982 to 2010.

Vegetation type data were obtained from a digitized 1:1 000 000 vegetation map of China. The vegetation was grouped into 10 types: needle leaf forests (2278 pixels), needle leaf and broadleaf mixed forests (279 pixels), broadleaf forests (7112 pixels), shrubs (3279 pixels), desert vegetation (2818 pixels), grasslands (12567 pixels), meadows (11528 pixels), marshes (1063 pixels), alpine vegetation (1535 pixels), and cultivated vegetation (19449 pixels) (Figure S1). Since phenology of cultivated vegetation is strongly impacted by human activities, we only focused on the natural vegetation in temperate China north of 30°N. We did not extend our study area into the south of 30°N because the evergreen vegetation over the humid tropics and subtropics show lack of seasonality and aberrant NDVI fluctuation related to non-vegetation weather impact (Kimball et al., 2004; Piao et al., 2006). Daily climate data were obtained from 486 meteorological stations across China.

Methods in determining spring green-up onset dates

We used the third generation GIMMS-NDVI3g data to retrieve the beginning of vegetation green-up onset date. In this study, five different methods (Gaussian-Midpoint,

Spline-Midpoint, HANTS-Maximum, Polyfit-Maximum, and Timesat-SG) were employed to estimate spring green-up onset date (Table 1).

For the Gaussian-Midpoint method (Gaussian thereafter), a Gaussian filter was used to filter the NDVI time series (Jonsson & Eklundh 2004; White *et al.* 2009; Wu *et al.* 2010a) and a dynamic threshold defined as NDVI ratio of 50% based on the annual minimum and maximum amplitude was employed to determine the green-up onset date (White *et al.* 1997, 2009; Yu *et al.* 2010). Using the same dynamic threshold with Gaussian method, Spline-Midpoint method (Spline hereafter) estimated the vegetation green-up onset date after reconstructing the daily NDVI time series by cubic-spline filter (White *et al.*, 2009). HANTS-Maximum method (HANTS hereafter) took use of Harmonic Analysis of Time Series (HANTS) model for NDVI time series reconstruction (Roerink *et al.*, 2000, 2003; Jakubauskas *et al.*, 2001). The threshold of this method was determined as the NDVI value with the highest positive relative change between the adjacent compositions, and the corresponding date was defined as the green-up onset date of the pixel (Lee *et al.*, 2002; Piao *et al.*, 2006; Jeong *et al.*, 2011). In Polyfit-Maximum method (Polyfit hereafter), the dynamic threshold is also defined as the highest positive relative change between two 15-days of the average NDVI series. The annual green-up onset date was then calculated as the interpolated NDVI crossed the threshold upwards via 6-degree polynomial regression (Piao *et al.*, 2006; Jeong *et al.*, 2011). Timesat-SG method (Timesat hereafter) used a Savitzky-Golay smoothing model for data filter (Chen *et al.*, 2004; Heumann *et al.*, 2007; White *et al.*, 2009; Brown *et al.*, 2010) and defined the NDVI value of the 20% seasonal amplitude from the

minimum level as the threshold (Jonsson & Eklundh 2004; White *et al.*, 2009; Brown *et al.*, 2010). Further details are given in Cong *et al.* (2012).

The trend in spring phenology was estimated by regressing spring green-up onset dates against year over the period 1982-2010. The negative and positive values indicated advance and delay in spring phenology, respectively.

Investigating the linkage between spring phenology and climate

To investigate the response of spring vegetation green-up date to the change in climate, we only considered four vegetation types (deciduous broadleaf forest, desert vegetation, grassland and meadows), which have more than ten meteorological stations. The NDVI value for each station is derived by averaging NDVI values over a window of 3 pixels by 3 pixels centered on each meteorological station. At each station, we performed correlation analyses between spring green-up onset date and pre-season climate variables (mean temperature and cumulative precipitation) over the last 29 years. We conducted sensitivity analyses to evaluate impacts of different pre-season period lengths (30, 60, 90, 120, 150 and 180 days) on spring phenology-climate relationship by the five methods used in quantifying spring green-up onset date. All pre-season periods were specified to end at the same date (Julian day: 128), which is calculated by averaging green-up onset dates from all years, stations and methods. Then we computed the mean temperature and cumulative precipitation of each pre-season period preceding this date for each year and each station. We used a 60-day pre-season period hereafter unless otherwise mentioned.

Results

Trends in spring green-up onset date

Regional scale analysis

Based on 29-year (1982-2010) GIMMS-NDVI3g data, we calculated the trends of spring green-up onset date over temperate China. All methods agreed on a negative trend (advance of spring phenology) over this period with method ensemble mean of -1.3 ± 0.6 days per decade (Figure 1). However, a large uncertainty was also found in trend values retrieved by different methods with a range of -0.4 and -1.9 days per decade (Figure 1). In terms of statistical significance, Gaussian (-1.9 days/decade, $P < 0.01$) and HANTS (-1.9 days/decade, $P < 0.01$) estimated larger and more significant advancing trends than Spline (-1.2 days/decade, $P = 0.06$) and Polyfit (-1.0 days/decade, $P = 0.05$) (Figure 1). By contrast, no significant trend was reported by Timesat method ($P = 0.51$).

Caution is needed, however, in comparing spring green-up onset dates from method ensemble. Gaussian and Spline methods systematically estimated later dates while HANTS and Timesat systematically predicted earlier dates (Figure 1).

Spatial patterns of trends in spring green-up onset date

Figure 2 displays spatial patterns of trend in spring green-up onset dates for five different methods, method ensemble and standard deviation (SD) calculated from the five methods. Over the whole study region, 60% of total pixels from method ensemble displayed an earlier shift in spring phenology, with a minimum value (57%) from HANTS and a

Accepted Article

maximum value (62%) from Spline. All methods except Polyfit indicated that pixels with advancing trends tended to increase along a latitudinal transect from Qinghai-Tibetan Plateau to Northeast China (Figure 2A-E). For example, North China Plain ($78\% \pm 3.8\%$), Inner Mongolia ($66\% \pm 5.5\%$) and mountains of Northeast China ($64\% \pm 3.5\%$) had a higher percentage of total pixels showing spring advance than Qinghai-Tibetan Plateau ($48\% \pm 8.4\%$). The values in parenthesis denoted method ensemble mean and standard deviation from the methods, except Polyfit. Furthermore, all methods agreed on a widespread advance in both mountains of Northeast China and North China Plain (Figure 2). Most of the pixels in these two regions showed spring advance between 1 and 5 days per decade and between 2 and 5 days per decade, respectively.

Although a spatial consistency in the sign of trend value was broadly observed, there was also appreciable uncertainty between methods in trend estimation, as measured by standard deviation of trend values from the five methods (Figure 2G). Most notably, in both Inner Mongolia and Qinghai-Tibetan Plateau, Polyfit estimated a widespread advance in spring phenology, but HANTS predicted a widespread delay. Thus, the SD of spring advance in most of the pixels in Inner Mongolia and northwest of Qinghai-Tibetan Plateau occurred between 2 and 5 days per decade and between 3 and 5 days per decade, respectively. In contrast, the pixels in relatively wet regions always had a smaller SD. For example, in mountains of Northeast China and southeast region in Qinghai-Tibetan Plateau, the SD of spring advance mostly ranged between 1 and 3 days per decade and between 0 and 3 days per decade, respectively.

Trends in spring green-up onset date for different vegetation types

Over the period 1982-2010, all methods consistently estimated negative trends (advance of spring phenology) in alpine vegetation (-2.1 ± 2.8 days per decade), shrubs (-2.1 ± 0.6 days per decade), needleleaf forests (-1.6 ± 0.7 days per decade), marshes (-1.4 ± 1.0 days per decade), meadows (-1.2 ± 0.5 days per decade) and grasslands (-0.7 ± 0.6 days per decade) (Figure 3a). The values in parenthesis denote method ensemble mean and standard deviation from the five methods. But a remarkable inter-method difference was still observed, and the most notable case was in alpine vegetation, with the trend value ranging from -0.4 to -7.0 days per decade. By contrast, we did not observe a consistent advancing trend (days per decade) across methods in deciduous broadleaf forests (-0.5 ± 2.2), needleleaf and broad leaf forests (0.0 ± 0.8) and desert vegetation (0.2 ± 1.1). In these three vegetation types, the five methods had opposite signs in estimation of spring phenological trend. For example, in deciduous broadleaf forests, HANTS method predicted a delayed trend in spring phenology (1.8 days per decade), contrary to advancing trends ($-0.9 \sim -1.9$ days per decade) by other methods.

In order to denote the spatial variability of the trend within each vegetation type, IQR (interquartile range) (days per decade) calculated as the difference between 75 and 25 percentile values was adopted. We found that forests (needleleaf forests: 2.2 ± 1.1 ; mixed forests: 3.4 ± 2.3 ; deciduous broadleaf forests: 3.7 ± 1.9) had the lowest IQR values. The vegetation types from arid and semi-arid regions (desert vegetation: 6.7 ± 2.2 , grasslands: 5.5 ± 2.0) had relatively higher values (Figure 3B). This suggested that the trend value was less

Accepted Article

spread in relatively wetter vegetation types. An inter-comparison of methods showed that methods differed in the retrieval of IQR values amongst vegetation types; for example, large inter-method discrepancy was found in desert vegetation, grasslands and alpine vegetation. Most notably, compared to other methods at mixed forests and deciduous broadleaf forests (2.1 ~ 2.6 and 2.3 ~ 3.5 days per decade), HANTS estimated much higher IQR values (7.6 and 6.9 days per decade) (Figure 3B).

Response of spring green-up onset date to climate change

Linkage between spring green-up onset date and climate

The correlation coefficient and the slope relating spring green-up date to pre-season climate (temperature and precipitation) as a surrogate of spring phenology sensitivity to climate are shown in Figure 5.

All methods agreed that green-up onset date was negatively correlated with pre-season mean temperature at widespread stations (Figure 4A). Across all stations, $69\% \pm 4\%$ of them had negative correlations (of which $35\% \pm 9\%$ were significantly negative) and $31\% \pm 4\%$ of them displayed positive correlations (of which $10\% \pm 2\%$ were significantly positive). In terms of vegetation type, deciduous broadleaf forests ($92\% \pm 11\%$) and meadows ($70\% \pm 11\%$) had a higher percentage of stations with negative correlations than grasslands ($64\% \pm 5\%$) and desert vegetation ($63\% \pm 9\%$). Regarding precipitation, $59\% \pm 11\%$ stations had a negative response of spring green-up onset date to pre-season cumulative precipitation (of which $6\% \pm 2\%$ stations were significantly negative) (Figure 4B). The remaining $41\% \pm 11\%$

Accepted Article

stations had positive responses (of which $9\% \pm 4\%$ stations were significantly positive). Grasslands ($61\% \pm 18\%$) and meadows ($61\% \pm 17\%$) had higher percentage of stations with negative responses than desert vegetation ($52\% \pm 6\%$) and deciduous broadleaf forests ($59\% \pm 12\%$). The “ \pm values” denote standard deviations calculated from the five methods. An inter-comparison of different methods suggested that inter-method discrepancy was larger in spring phenology responses to cumulative pre-season precipitation than that in spring phenology responses to mean pre-season temperature.

As shown in Figure 5A, temperature sensitivities (days/ $^{\circ}$ C) of deciduous broadleaf forests (-2.1 ± 0.7) and meadows (-1.9 ± 1.8) with relatively abundant soil moisture was stronger than those of grasslands (-1.0 ± 0.9) and desert vegetation (-0.4 ± 0.8) in arid and semi-arid region. Regarding precipitation sensitivity (days/100 mm), deciduous broadleaf forests and grasslands had precipitation sensitivities of -1.2 ± 4.3 and -1.5 ± 8.6 respectively. In contrast, positive precipitation sensitivity (delay of spring phenology with precipitation increase) was found in desert vegetation (0.7 ± 9.2) and meadows (4.2 ± 16.3). In terms of spring phenological sensitivity to climate (precipitation and temperature), an inter-comparison of the five methods indicated that a relatively large spread of values was always found in Polyfit and HANTS methods when all stations were taken into account (Figure 5). At the level of vegetation type, a large data spread was found in desert vegetation and grasslands by HANTS method, and a similar spread was detected in meadows by Polyfit. In contrast, the inter-method discrepancy was found to be the smallest in deciduous broadleaf forests.

Temperature sensitivity of spring green-up onset date vs. precipitation

In order to understand how precipitation affected temperature sensitivity of spring phenology, we performed correlation analysis between temperature sensitivity of spring phenology and cumulative pre-season precipitation across all stations (Figure 6) and stations within each vegetation type (Table 2). According to method ensemble, we found that temperature responses of spring phenology significantly became stronger with increasing cumulative pre-season precipitation across all stations ($r = -0.3$, $p < 0.01$). The same conclusion was reached by all approaches except HANTS and Polyfit with non-significant slope ($p > 0.05$) (Figure 6). In terms of stations within vegetation type, besides Polyfit method at three vegetation types (deciduous broadleaf forests, grasslands and meadows), the negative correlation between temperature sensitivity of spring phenology and cumulative pre-season precipitation was also found by all other methods (Table 2). But the significant ($p < 0.05$) or marginally significant ($p < 0.10$) correlation was mainly concentrated in forests and meadows.

Finally, as the length of pre-season period went beyond 120 days, all the methods indicated that the number of stations with negative spring phenology-temperature correlation was significantly reduced. This phenomenon was notable for deciduous broadleaf forests and meadows (Table S1, S2). Unlike temperature, for each vegetation type, the percentage of stations with negative (or positive) spring phenology-precipitation correlation did not significantly change with different lengths of pre-season (30, 90, 120, 150 and 180 days), which was also found by all the five methods (Table S1, S2).

Discussion

Change in spring green-up onset date

Over temperate China, the average spring green-up onset date derived from five methods showed that spring vegetation green-up date has advanced by 1.3 ± 0.6 days per decade from 1982 to 2010. This estimation is smaller than the result (-1.9 days per decade) of Ma & Zhou (2012), but much less than the estimation (-7.9 days per decade) from Piao et al. (2006). The discrepancy becomes less if the same study period is fixed. For example, if we consider only the period of 1982-2006, our estimate of spring phenological trend (-1.7 days per decade) was closer to that of Ma & Zhou (2012). This demonstrated that the differences in trend estimation across studies were partly related to the study period (Badeck *et al.*, 2004; Zhu *et al.*, 2011).

It has also been suggested that the magnitudes of the satellite derived phenological trends differ dramatically among studies because of the different methods used to retrieve spring vegetation green-up date (White *et al.* 2009). For instance, applying the Timesat Method, Zeng et al. (2011) estimated that spring vegetation green-up date over North America has advanced by about 0.3 days per decade, which is only 20% of the advanced rate (-1.3 days per decade) derived by Zhu et al. (2011) based on Piecewise logistic method. Our results also support that methods could induce large uncertainties in the magnitude of trends inferred from satellite-based vegetation phenology, although the overall patterns in vegetation green-up date trends from the five methods we used were relatively consistent. The largest earlier trend of vegetation green-up date (1.9 days/decade) detected by the Gaussian and

HANTS methods are about 5 times of that by the Timesat method (0.4 days/decade). This inter-method inconsistency in trend estimation has also been documented in prior studies (e.g. White *et al.*, 2009). The discrepancy can be expected because methods differ in noisy filter function in NDVI time series reconstruction and critical thresholds in determining spring green-up onset date (see also Cong *et al.*, 2012). For example, Timesat method, which relies on 20% NDVI amplitude threshold for phenology determination, could be unstable for those ecosystem types with smaller NDVI amplitudes because it has the limitations in identifying the minimum NDVI clearly (Chen *et al.*, 2004). Moreover, the uncertainty in trend estimation induced by methods was vegetation type-dependent, and large spread of trend values across different methods was always found in vegetation types of areas with low precipitation (e.g. desert vegetation and grasslands). This is partly related to the impact of bare soil on satellite signal.

Responses of spring green-up onset date to climate change

Our multi-method analysis indicated clear negative responses of spring vegetation green-up date to mean preseason temperature at most of the meteorological stations, which was consistent with previous findings (White *et al.*, 1999; Beaubien & Freeland 2000; Kramer *et al.*, 2000; Sparks *et al.*, 2000; Piao *et al.*, 2006; Menzel *et al.* 2006; Zeng *et al.*, 2011; Cong *et al.*, 2012). In general, spring phenology was most significantly correlated to the mean temperature occurring 2-3 months before the mean green-up onset date (Julian day: 128), which was comparable to Piao *et al.* (2006). Based on mean green-up onset date calculated from the five methods (black boxplot indicated in Figure 5), the temperature

Accepted Article

response varied between -9.7 days/°C and 6.3 days/°C with a mean response of -1.2 days/°C across all stations. We did observe some stations with delayed spring phenology to increasing temperature. It is possible since less frequent chilling early in the growing season could extend the time necessary for chilling cues to be met (Zhang *et al.*, 2007; Körner & Balsler 2010; Yu *et al.*, 2010). This is also likely associated with drought stress at the spring green-up onset date, which is probably site- or vegetation-dependent.

In contrast to temperature, most of the correlation between spring phenology and precipitation was found to be non-significant. This suggests that variation of spring phenology was mainly driven by changes in temperature or other precipitation characteristics (e.g. timing of precipitation) rather than pre-season precipitation. It was expected that spring phenology responses to precipitation would not be significant over a majority of stations in meadows and deciduous broadleaf forests receiving relatively abundant precipitation. However, in both grasslands and desert vegetation, where precipitation was supposed to be an important determinant for plant growth (e.g. Abd El-Ghani 1997; Ghazanfar 1997), we also rarely observed significant influence of cumulative pre-season precipitation on spring green-up onset date. Such insensitivity to precipitation amount did not negate impacts of other precipitation characteristics (e.g. first timing of precipitation) on spring phenology. For example, in the semi-arid, drought-deciduous ecosystems in the Kalahari region of South Africa, Jolly and Running (2004) found that predictions of leaf flushing timing was better using the first significant precipitation event at Maun than at Tshane site. Ghazanfar (1997) also documented that late precipitation delayed the onset of all phenological phases in all

life-forms from a gravel desert Wadi in northern Oman. However, this needs to be further explored in a future study.

Direct evidence was lacking for significant influences of cumulative pre-season precipitation on spring green-up onset date. But our cross-station analysis between temperature sensitivity of spring phenology and cumulative pre-season precipitation indicated that spring green-up onset showed increasing advance in response to pre-season temperature as pre-season precipitation increased. For example, there were larger proportions of stations in deciduous broadleaf forests and meadows with more precipitation than those in grasslands and desert vegetation with less precipitation. This is possibly related to the fact that temperature control of plant growth became stronger if the soil moisture constraints were released in relatively wetter locations. It has implications for understanding the responses of spring phenology to climate change since shifts in precipitation will be expected to occur in concert with increasing temperatures (IPCC 2007). If our cross-site result was extrapolated from space to time, the sensitivity of spring green-up onset date to temperature would increase to 3.6 ± 2.3 days/ $^{\circ}\text{C}$ given the increase of precipitation by 100mm. However, we should note that if this cross-station analysis was performed at each vegetation type, temperature sensitivity of spring phenology did not significantly respond to cumulative precipitation in desert vegetation and grasslands. On the one hand, this might be related to the possibility that much of the rainwater was lost to evaporation within a few days after rainfall and could not be stored in the soil (Kondo & Xu 1996; Zhao & Running 2010). On the other hand, the green-up onset especially in desert vegetation could be more regulated by snowmelt

Accepted Article

or first rainfall (Xu et al., 2009) than by the cumulative precipitation amount. However, future in-situ studies are still needed to validate our results.

Acknowledgements

This study was supported by the National Natural Science Foundation of China (grant 41125004 and 30970511) and Chinese Ministry of Environmental Protection Grant (201209031).

References

Abd El-Ghani MM (1997) Phenology of ten common plant species in western Saudi Arabia.

Journal of Arid Environments, **35**, 673-683.

Asrar G, Fuchs M, Kanemasu ET, Hatfield JL (1984) Estimating absorbed photosynthetically active radiation and leaf area index from spectral reflectance in wheat. *Agronomy Journal*, **76**, 300-306.

Badeck FW, Bondeau A, Böttcher K, Doktor D, Lucht W, Schaber J, Sitch S (2004)

Responses of spring phenology to climate change. *New Phytologist*, **162**, 295-309.

Baldocchi D, Falge E, Gu LH et al. (2001) Fluxnet : A new tool to study the temporal and spatial variability of ecosystem-scale carbon dioxide, water vapor, and energy flux densities. *Bulletin of the American Meteorological Society*, **82**, 2415-2434.

Beaubien EG, Freeland HJ (2000) Spring phenology trends in Alberta, Canada: links to ocean temperature. *International Journal of Biometeology*, **44**, 53-39.

Brown ME, De Beurs K, Vrieling A (2010) The response of African land surface phenology to large scale climate oscillations. *Remote Sensing of Environment*, **114**, 2286-2296.

- Chen, J, Jönsson, P, Tamura, M, Gu, ZH, Matsushita, B, Eklundh, L (2004) A simple method for reconstructing a high-quality NDVI time-series data set based on the Savitzky-Golay filter. *Remote Sensing of Environment*, **91**, 332-344.
- Chen XQ, Hu B, Yu R (2005) Spatial and temporal variation of phenological growing season and climate change impacts in temperate eastern China. *Global Change Biology*, **11**, 1118-1130.
- Cleland EE, Chuine I, Menzel A, Mooney HA, Schwartz MD (2007) Shifting plant phenology in response to global change. *Trends in Ecology & Evolution*, **22**, 357-365.
- Cong N, Piao SL, Chen AP et al. (2012) Spring vegetation green-up date in China inferred from SPOT NDVI data: A multiple model analysis. *Agricultural and Forest Meteorology*, **165**, 104-113.
- Fang XQ, Yu WH (2002) Progress in the studies on the phenological responding to global warming. *Advance in Earth Sciences*, **17**, 714-719 (in Chinese).
- Ghazanfar (1997) The phenology of desert plants: a 3-year study in a gravel desert wadi in northern Oman. *Journal of Arid Environments*, **35**, 407-417.
- Heumann, BW, Seaquist, JW, Eklundh, L, Jönsson, P (2007) AVHRR derived phenological change in the Sahel and Soudan, Africa, 1982-2005. *Remote Sensing of Environment*, **108**, 385-392.
- Hu J, Moore DJP, Burns SP, Monson RK (2010) Longer growing seasons lead to less carbon sequestration by a subalpine forest. *Global Change Biology*, **16**, 771-783.
- IPCC (Intergovernmental Panel on Climate Change) (2007) *Climate Change 2007: The scientific basis*. Cambridge University Press, New York.

- Jakubauskas ME, Legates DR, Kastens JH (2001) Harmonic analysis of time-series AVHRR NDVI data. *Photogrammetric Engineering & Remote Sensing*, **67**, 461-470.
- Jeong SJ, Ho CH, Gim HJ, Brown ME (2011) Phenology shifts at start vs. end of growing season in temperate vegetation over the Northern Hemisphere for the period 1982-2008. *Global Change Biology*, **17**, 2385-2399.
- Jolly WM, Running SW (2004) Effects of precipitation and soil water potential on drought deciduous phenology in the Kalahari. *Global Change Biology*, **10**, 303-308.
- Jonsson P, Eklundh L (2004) TIMESAT – a program for analyzing time-series of satellite sensor data. *Computers & Geosciences*, **30**, 833-845.
- Keeling CD, Chin JFS, Whorf TP (1996) Increased activity of northern vegetation in inferred from atmospheric CO₂ measurements. *Nature*, **382**, 146-149.
- Kimball JS, McDonald KC, Running SW, Frohling SE (2004) Satellite radar remote sensing of seasonal growing seasons for boreal and subalpine evergreen forests. *Remote Sensing of Environment*, **90**, 243-258.
- Kondo J, Xu JQ (1996) Seasonal variations in the heat and water balances for nonvegetated surfaces. *Journal of Applied Meteorology*, **36**, 1676-1685.
- Körner C, Basler D (2010) Phenology under global warming. *Science*, **327**, 1461-1462.
- Kramer K, Leinonen I, Loustau D (2000) The importance of phenology for the evaluation of impact of climate change on growth of boreal, temperate and Mediterranean forests ecosystems: an overview. *International Journal of Biometeorology*, **44**, 67-75.
- Lee R, Yu F, Price KP, Ellis J, Shi P (2002) Evaluating vegetation phenological patterns in Inner Mongolia using NDVI time-series analysis. *International Journal of Remote*

Sensing, **23**, 2505-2512.

Ma T, Zhou CH (2012) Climate-associated changes in spring plant phenology in China.

International Journal of Biometeorology, **56**, 269-275.

Menzel A, Fabian P (1999) Growing season extended in Europe. *Nature*, **397**, 659-659.

Menzel A, Sparks TH, Estrella N et al. (2006) European phenological response to climate change matches the warming pattern. *Global Change Biology*, **12**, 1969-1976.

Niemand C, Kostner B, Prasse H, Grunwald T, Bemhofer C (2005) Relatin tree phenology with annual carbon fluxes at Tharandt forest. *Meteorologische Zeitschrift*, **14**, 196-202.

Parmesan C (2006) Ecological and evolutionary responses to recent climate change. *Annual Review of Ecology Evolution and Systematics*, **37**, 637-669.

Parmesan C, Yohe G (2003) A globally coherent fingerprint of climate change impacts across natural systems. *Nature*, **421**, 37-42.

Peng SS, Chen AP, Xu L, et al. (2011) Recent change of vegetation growth trend in China. *Environmental Research Letters*, **6**, 044027, doi:10.1088/1748-9326/6/4/044027.

Peñuelas J, Rutishauser T, Filella I (2009) Phenology feedbacks on climate change. *Ecology*, **324**, 887-888.

Piao SL, Ciais P, Friedlingstein P, et al. (2008) Net carbon dioxide losses of northern ecosystems in response to autumn warming. *Nature*, **451**, 49-53.

Piao SL, Fang JY, Zhou LM, Ciais P, Zhu B (2006) Variations in satellite-derived phenology in China's temperate vegetation. *Global Change Biology*, **12**, 672-685.

Piao SL, Friedlingstein P, Ciais P, Viovy N, Demarty J (2007) Growing season extension and its effects on terrestrial carbon flux over the last two decades. *Global Biogeochemical*

Cycles, **21**, GB3018, doi:10.1029/2006GB002888.

Piao SL, Ciais P, Huang Y, et al. (2010) The impacts of climate change on water resources and agriculture in China. *Nature*, **467**, 43-51.

Richardson AD, Black TA, Ciais P, et al. (2010) Influence of spring and autumn phenological transitions on forest ecosystem productivity. *Philosophical Transactions of the Royal Society*, **365**, 3227-3246.

Roerink GJ, Menenti M, Soepboer W, Su Z (2003) Assessment of climate impact on vegetation dynamics by using remote sensing. *Physics and Chemistry of the Earth*, **28**, 103-109.

Roerink GJ, Menenti M, Verhoef W (2000) Reconstructing cloudfree NDVI composites using Fourier analysis of time series. *International Journal of Remote Sensing*, **21**, 1911-1917.

Sparks TH, Jeffree EP, Jeffree CE (2000) An examination of the relationship between glowering times and temperature at the national scale using long-term phenological records from the UK. *International Journal of Biometeorology*, **44**, 82-87.

Schwartz MD (1998) Green-wave phenology. *Nature*, **394**, 839-840.

Stöckli R, Rutishauser T, Baker I., Liniger MA, Denning AS (2011) A global reanalysis of vegetation phenology. *Journal of Geophysical Research*, **116(G03020)**, doi:10.1029/2010JG001545.

Stöckli R, Rutishauser T, Dragoni D, et al., (2008) Remote sensing data assimilation for a prognostic phenology model, *Journal of Geophysical Research-Biogeosciences*, **113(G4)**, doi: 10.1029/2008JG000781.

Tao F, Yokozawa M, Xu Y, Hayashi Y, Zhang Z (2006) Climate changes and trends in

phenology and yields of field crops in China 1982-2000. *Agricultural and Forest Meteorology*, **138**, 82-92.

Tucker CJ, Pinzon JE, Brown ME et al. (2005) An extended AVHRR 8-km NDVI dataset compatible with MODIS and SPOT vegetation NDVI data. *International Journal of Remote Sensing*, **26**, 4485-4498.

Vitasse Y, Porté AJ, Kremer A, Michalet R, Delzon S (2009) Responses of canopy duration to temperature changes in four temperate tree species: relative contributions of spring and autumn leaf phenology. *Oecologia*, **161**, 187-198.

Wang XH, Piao SL, Ciais P, Li J, Friedlingstein P, Koven C, Chen AP (2011) Spring temperature change and its implication in the change of vegetation growth in North America from 1982 to 2006. *Proceedings of the National Academy of Sciences of the United States of America*, **108**, 1240-1245.

White MA, deBeurs KM, Didan K, et al. (2009) Intercomparison, interpretation, and assessment of spring phenology in North America estimated from remote sensing for 1982-2006. *Global Change Biology*, **15**, 2335-2359.

White MA, Running SW, Thornton PE (1999) The impact of growing-season length variability on carbon assimilation and evapotranspiration over 88 years in the eastern US deciduous forest. *International Journal of Biometeorology*, **42**, 139-145.

White MA, Thornton PE, Running SW (1997) A continental phenology model for monitoring vegetation responses to interannual climatic variability. *Global Biogeochemical Cycles*, **11**, 217-234.

Wu WB, Yang P, Tang HJ, Zhou QB, Chen ZX, Shibasaki R (2010) Characterizing spatial

patterns of phenology in cropland of China based on remotely sensed data. *Agricultural Sciences in China*, **9**, 101-112.

Xu JC, Grumbine RE, Shrestha A, Eriksson M, Yang XF, Wang Y, Wilkes A (2009) The melting Himalayas: Cascading effects of climate change on water, biodiversity, and livelihoods. *Conservation Biology*, **23**, 520-530.

Yu HY, Luedeling E, Xu JC (2010) Winter and spring warming result in delayed spring phenology on the Tibetan Plateau. *Proceedings of the National Academy of Sciences of the United States of America*, **107**, 22151-22156.

Zeng HQ, Jia GS, Epstein H (2011) Recent changes in phenology over the northern high latitudes detected from multi-satellite data. *Environmental Research Letters*, **6**, doi: 10.1088/1748-9326/6/4/045508.

Zhang XY, Tarpley D, Sullivan T (2007) Diverse responses of vegetation phenology to a warming climate. *Geophysical Research Letters*, **34(L19405)**, doi: 10.1029/2007GL031447.

Zhao MS, Running SW (2010) Drought-induced reduction in global terrestrial net primary production from 2000 through 2009. *Science*, **329**, 941-943.

Zheng JY, Ge QS, Hao ZX (2002) Impacts of climate warming on plants phenophases in China for the last 40 years. *Chinese Science Bulletin*, **47**, 1826-1831.

Zhou LM, Tucker C, Kaufmann R, Slayback D, Shabanov N, Myneni R (2001) Variations in northern vegetation activity inferred from satellite data of vegetation index during 1981 to 1999. *Journal of Geophysical Research-Atmospheres*, **106**, 20069-20083.

Zhu WQ, Tian HQ, Xu XF, Pan YZ, Chen GS, Lin WP (2012) Extension of the growing

season due to delayed autumn over mid and high latitudes in North America during 1982-2006. *Global Ecology and Biogeography*, **21**, 260-271.

Table 1 Summary of five methods in determining spring vegetation green-up onset dates from satellite-derived NDVI data

Method	Data filter function	Threshold determination
Gaussian	$NDVI(t) = a + b \times e^{-((t-c)/d)^2}$	Midpoint
Spline	$NDVI(t) = a_1 t^3 + b_1 t^2 + c_1 t + d_1$	Midpoint
HANTS	$NDVI(t) = a_0 + \sum_{i=1}^n a_i \cos(\omega_i t - \phi_i)$	Maximum variation
Polyfit	$NDVI(t) = a_0 + a_1 t + a_2 t^2 + a_3 t^3 + \dots + a_n t^n$	Maximum variation
Timesat	$NDVI(t) = \frac{\sum_{i=-m}^{i=m} C_i NDVI_{j+i}}{N}$	20% of NDVI amplitude

Data filter function was used to reconstruct NDVI time series by smoothing out the noise due to cloud contamination and atmospheric variability. Threshold was then adopted to determine spring green-up onset date from reconstructed NDVI time series. In the data filter function, t is the Julian date, $NDVI(t)$ is the fitted NDVI value by the equation of each filter function. For Timesat method, N is the number of convoluting integers which is equal to the smoothing window size, and j is the running index of the original ordinate data table.

Table 2 Slope of temperature sensitivity of spring vegetation green-up date versus cumulative pre-season precipitation in different vegetation types. The pre-season period (60-day period) was defined the same with Figure 4. † indicated $P < 0.1$, * indicated $P < 0.05$, and ** indicated $P < 0.01$. DBF is deciduous broadleaf forests, Desert is desert vegetation, GRA is grasslands.

Method	Vegetation			
	DBF	Desert	GRA	Meadows
Gaussian	-0.04 [†]	-0.05	-0.03	-0.05 ^{**}
Spline	-0.03 [*]	-0.02	-0.02	-0.10 ^{**}
HANTS	-0.06	-0.07	-0.05	-0.01
Polyfit	0.02	-0.05	0.04	0.04
Timesat	-0.02	-0.24 [†]	-0.02	-0.07 ^{**}
MEAN	-0.03 [*]	-0.07 [†]	-0.01	-0.05 ^{**}

Figure legends

Figure 1 Interannual variation in spring vegetation green-up onset date from 1982 to 2010 over the temperate China. Five different methods were applied. The unit of slope is days per decade.

Figure 2 Spatial patterns of trend in spring green-up onset date from 1982 to 2010. We applied five different methods: (a) Gaussian; (b) Spline; (c) HANTS; (d) Polyfit; (e) Timesat; and (f) their ensemble mean. The standard deviation of trends from the five methods on the spatial scale was displayed in panel G. The negative value indicates advance trend in spring green-up dates.

Figure 3 (a) Average and (b) interquartile range (IQR) of trend in spring vegetation green-up onset date for different vegetation types. Interquartile range (IQR) was calculated as the difference between 75 and 25 percentile values to denote the variability in trend values within each vegetation type. The error bar indicated the standard deviation from the five methods.

NF is needleleaf forests, MF is needleleaf and broadleaf forests, DBF is deciduous broadleaf forests, Desert is desert vegetation, GRA is grasslands, and Alpine is alpine vegetation.

Figure 4 Correlation coefficients (r) between onset date of green-up and (a) mean preseason temperature and (b) cumulative preseason precipitation at different vegetation types for the five methods and method ensemble mean. The preseason period was defined as 60 days before mean spring green-up onset date (Julian day 128) calculated across all stations, years and methods. Dashed line indicated zero correlation coefficient, and n was the number of stations within each vegetation type.

Figure 5 The sensitivity (s) of spring green-up onset date to (a) mean preseason temperature and (b) cumulative preseason precipitation for the five methods and method ensemble mean. The sensitivity value was the linear slope relating green-up onset date to preseason climate (temperature and precipitation). The preseason period (60-day period) was defined the same with Figure 4. Dashed lines show zero value, and n is the number of stations within each vegetation type.

Figure 6 Relationship between temperature sensitivity of green-up onset (days/°C) and preseason precipitation (mm) across 181 meteorological stations. We applied five different methods: (a) Gaussian; (b) Spline; (c) HANTS; (d) Polyfit; (e) Timesat; and (f): their ensemble mean. The preseason period (60-day period) was defined the same with Figure 4.

Figure 1

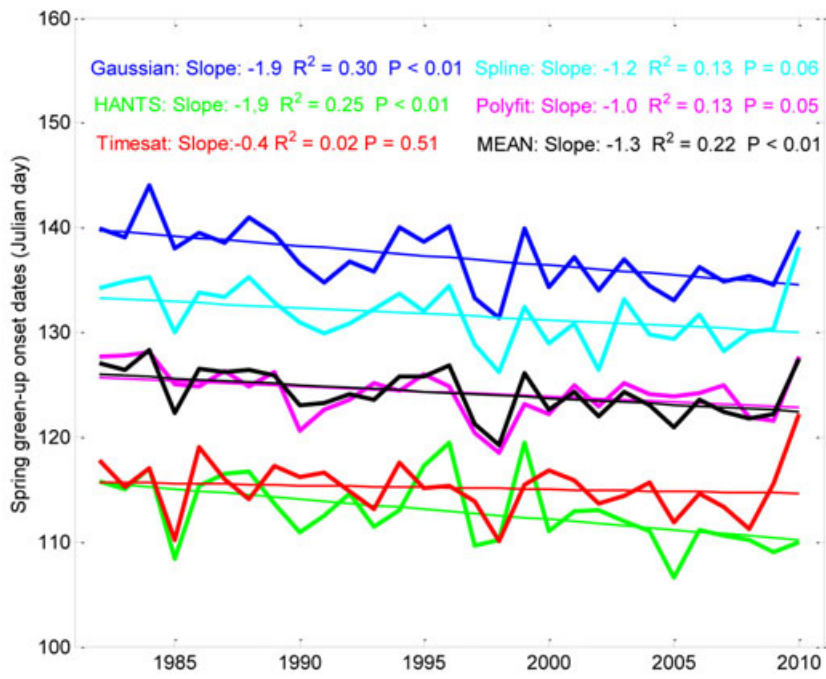


Figure 2

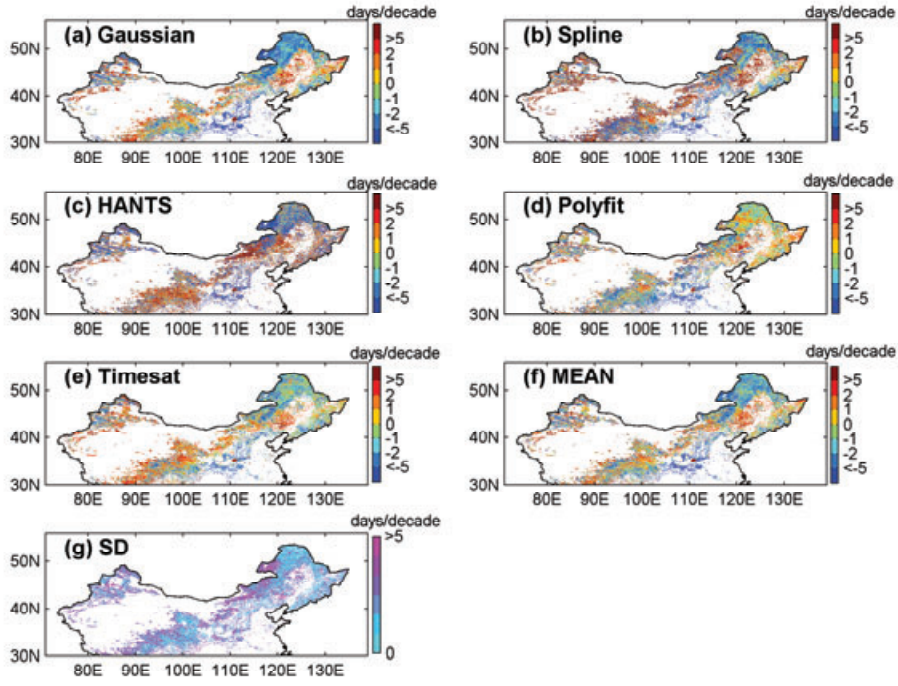


Figure 3

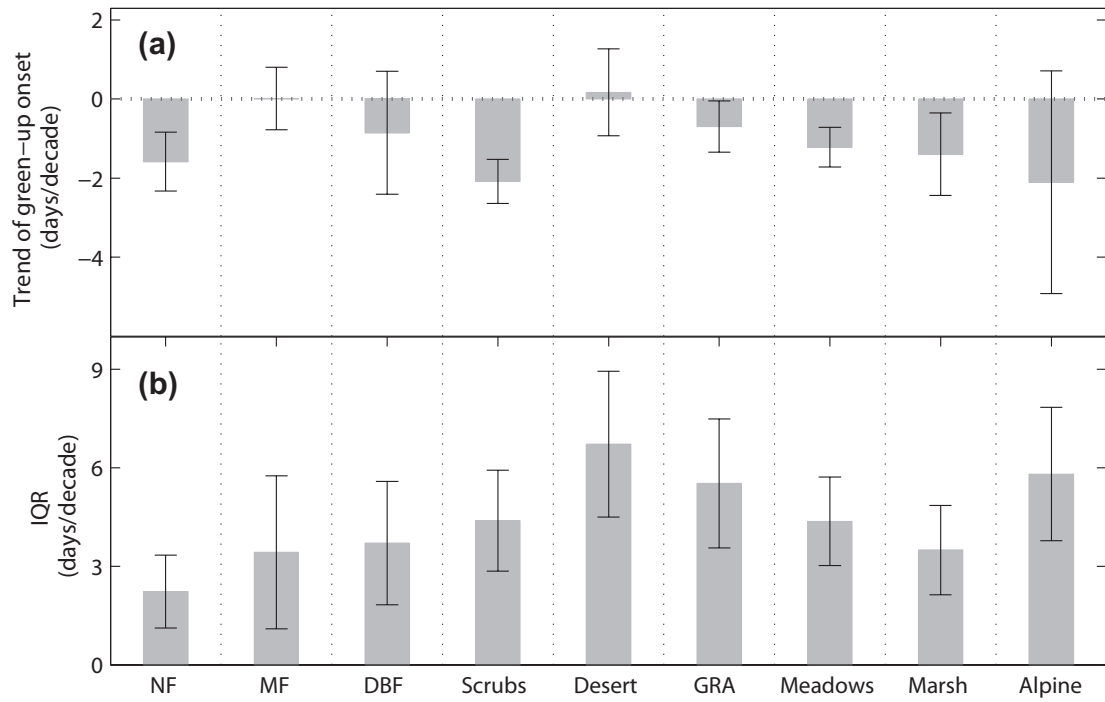


Figure 4

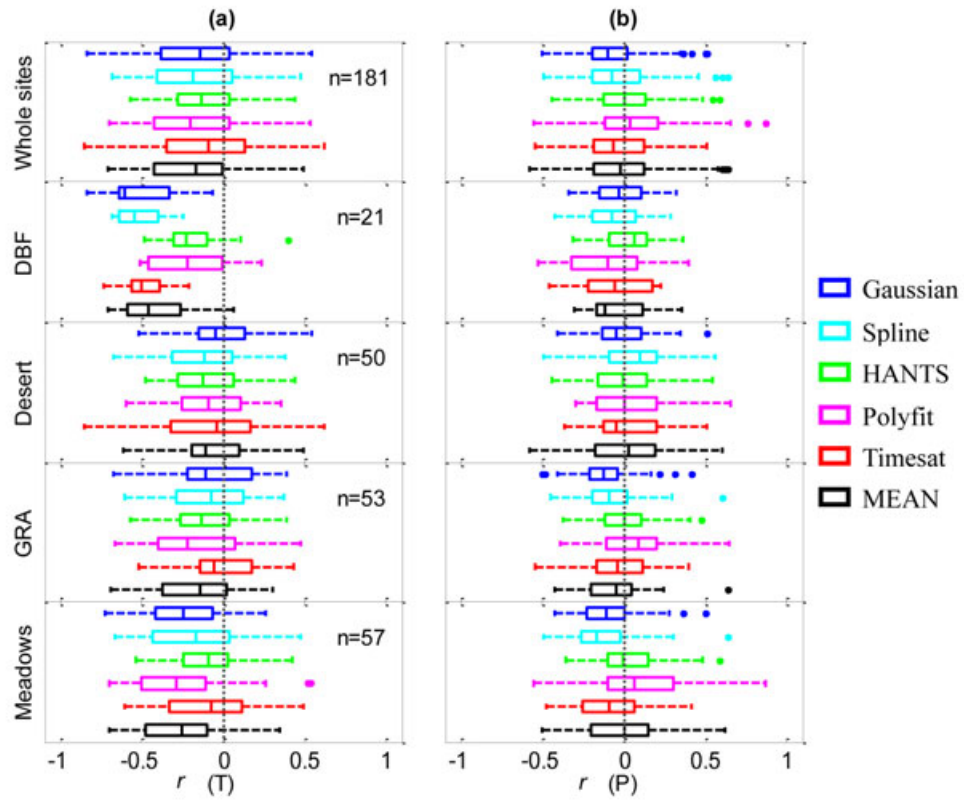


Figure 5

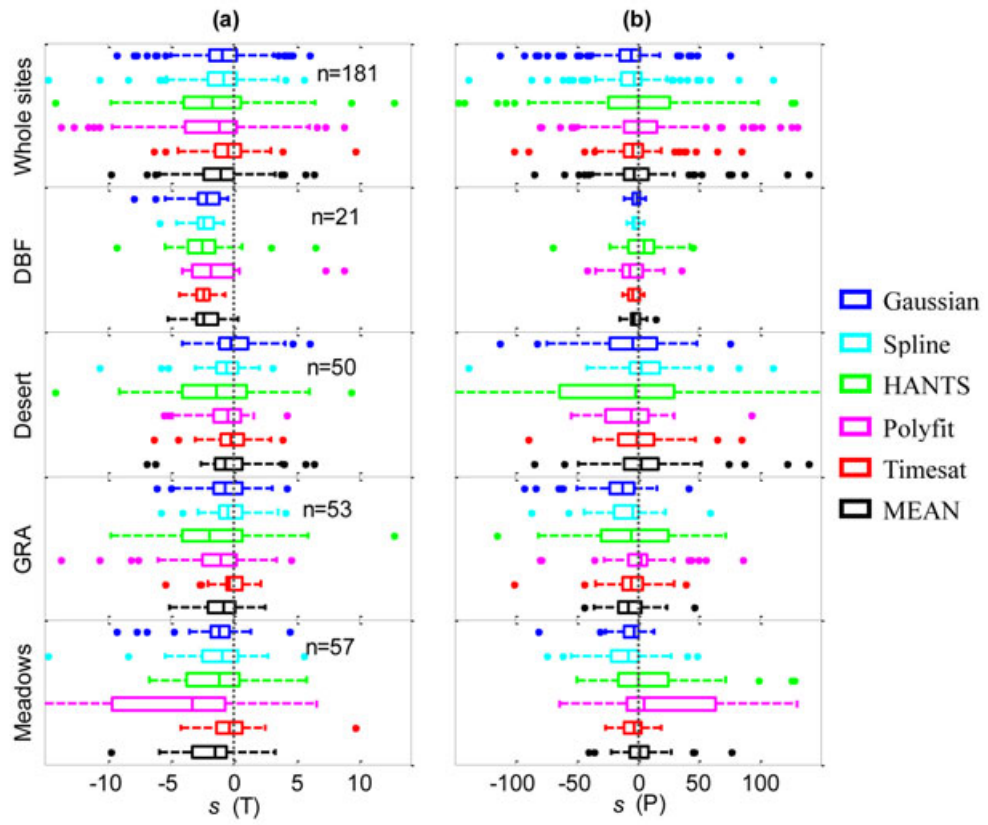


Figure 6

